RNA-seq of spinal cord from nerve-injured rats after spinal cord stimulation

Kimberly E Stephens[1,2,3], Zhiyong Chen[3,4], Eellan Sivanesan[3],
Srinivasa N Raja[3], Bengt Linderoth[5], Sean D Taverna[1,2], and
Yun Guan[3,6]

Abstract

Spinal cord stimulation has become an important modality in pain treatment especially for neuropathic pain conditions refractory to pharmacotherapy. However, the molecular control of inhibitory and excitatory mechanisms observed after spinal cord stimulation are poorly understood. Here, we used RNA-seq to identify differences in the expression of genes and gene networks in spinal cord tissue from nerve-injured rats with and without repetitive conventional spinal cord stimulation treatment. Five weeks after chronic constrictive injury to the left sciatic nerve, male and female rats were randomized to receive repetitive spinal cord stimulation or no treatment. Rats receiving spinal cord stimulation underwent epidural placement of a miniature stimulating electrode and received seven sessions of spinal cord stimulation (50 Hz, 80% motor threshold, 0.2 ms, constant current bipolar stimulation, 120 min/session) over four consecutive days. Within 2 h after the last spinal cord stimulation treatment, the L4-L6 spinal segments ipsilateral to the side of nerve injury were harvested and used to generate libraries for RNA-seq. Our RNA-seq data suggest further increases of many existing upregulated immune responses in chronic constrictive injury rats after repetitive spinal cord stimulation, including transcription of cell surface receptors and activation of non-neuronal cells. We also demonstrate that repetitive spinal cord stimulation represses transcription of several key synaptic signaling genes that encode scaffold proteins in the post-synaptic density. Our transcriptional studies suggest a potential relationship between specific genes and the therapeutic effects observed in patients undergoing conventional spinal cord stimulation after nerve injury. Furthermore, our results may help identify new therapeutic targets for improving the efficacy of conventional spinal cord stimulation and other chronic pain treatments.

Keywords

RNA-seq, gene expression, spinal cord stimulation, nerve injury, pain, spinal cord

Date Received: 2 October 2018; revised: 28 October 2018; accepted: 12 November 2018

Introduction

Increased efforts to avoid the severe side effects known to opioid analgesics are shifting treatment for chronic pain conditions towards non-opioid and interventional therapies. A mounting body of evidence supports the use of spinal cord stimulation (SCS) for its treatment effectiveness and safety.[1–5] Conventional SCS was developed

[4]Institute of Basic Medical Sciences, Department of Human Anatomy, Histology and Embryology, Neuroscience Center, Chinese Academy of Medical Sciences, School of Basic Medicine, Peking Union Medical College, Beijing, China
[5]Division of Functional Neurosurgery, Department of Clinical Neuroscience, Karolinska Institutet, Stockholm, Sweden
[6]School of Medicine, Department of Neurological Surgery, Johns Hopkins University, Baltimore, MA, USA

Corresponding Authors:
Yun Guan, Division of Pain Medicine, Department of Anesthesiology and Critical Care Medicine, Johns Hopkins University School of Medicine, 720 Rutland Ave., Ross 350, Baltimore, MD 21205, USA.
Email: yguan1@jhmi.edu
Sean D. Taverna, Department of Pharmacology and Molecular Sciences and the Center for Epigenetics, Johns Hopkins University School of Medicine, 855 N. Wolfe Street, Rangos 575, Baltimore, MD 21205, USA.
Email: staverna@jhmi.edu

[1]Department of Pharmacology and Molecular Sciences, School of Medicine, Johns Hopkins University, Baltimore, MA, USA
[2]Center for Epigenetics, School of Medicine, Johns Hopkins University, Baltimore, MA, USA
[3]Department of Anesthesia and Critical Care Medicine, School of Medicine, Johns Hopkins University, Baltimore, MA, USA

based on the seminal "gate control" theory of pain[6] and remains a widely used neurostimulation pain therapy. Conventional SCS involves placement of epidural leads, often at a few levels above (i.e., rostral to) the affected spinal segments that receive noxious inputs (e.g. "pain segments"), and delivery of pulsed electricity to stimulate the dorsal column. Conventional SCS activates low-threshold afferents (i.e., Aβ-fibers) which produces the mild paresthesia (i.e., tingling sensation). Thus, pain inhibition from conventional SCS partially acts through antidromic action potentials in dorsal column fibers to activate inhibitory mechanisms in distal "pain segments" via collateral branches.[7,8]

Pain inhibitory effects by conventional SCS are intricately linked with spinal mechanisms,[9–11] as evident by inhibition of neuronal sensitization and nociceptive transmission at spinal level, and changes in release of neurotransmitters and neuromodulators in the spinal cord.[11–14] However, the molecular mechanisms which underlie the therapeutic effects of SCS remain unknown. While limited in scope, previous findings suggest that SCS induces broad and prolonged changes in gene expression.[15–17] To identify new gene networks and molecular pathways altered after repetitive SCS, we conducted the first RNA-seq study of the lumbar spinal cord after repetitive SCS at the T13-L1 level in rats during the maintenance phase of neuropathic pain. To mimic clinical SCS, we applied bi-polar stimulation through a miniature quadripolar electrode which has been validated in previous studies.[12,14,18,19] Our findings are consistent with previous reports of an increased immune response associated with SCS. Notably, we also identified downregulation of several genes encoding scaffold proteins located on the postsynaptic membrane in nerve-injured rats after SCS for the first time, which may impact neurotransmission and synaptic efficacy associated with central sensitization. Such transcriptional studies will help explain physiological changes that occur in the spinal cord following repeated SCS after nerve injury and may identify novel therapeutic targets which improve the efficacy of SCS.

Methods

Animals

Adult male and female Sprague-Dawley rats ($n = 12$; 12–16 weeks old; Harlan Bioproducts for Science, Indianapolis, IN) were allowed to acclimate for a minimum of 48 h prior to any experimental procedure. The rats were housed separately after implanting the SCS electrode and given access *ad libitum* to food and water. All procedures involving animals were reviewed and approved by the Johns Hopkins Animal Care and are performed in accordance with the NIH Guide for the Care and Use of Laboratory Animals.

Behavior testing

Mechanical hypersensitivity was measured using von Frey monofilaments as previously described.[12,20] Animals were placed in individual plexiglass cages with a wire mesh floor and allowed to acclimate for 1 h. Response to tactile stimulation to the midplantar surface of the hind paw ipsilateral to the nerve lesion was determined with the up-down method using a series of von Frey monofilaments (0.38, 0.57, 1.23, 1.83, 3.66, 5.93, 9.13, and 13.1 g) as described previously.[20] Each monofilament was applied for 4 to 6 s to the test area between the footpads on the plantar surface of each hind paw. Monofilaments with increasing force were applied until a positive response was observed (e.g., abrupt paw withdrawal, shaking, and licking). When a positive response was observed, the monofilament with the next lower force was applied. If a negative response was observed, the next higher force was used. The test continued (1) for five filament applications after a positive test was observed or (2) until the upper or lower end of the von Frey monofilament set was reached. The paw withdrawal threshold (PWT) was determined according to the formula provided by Dixon.[21] If a rat did not achieve at least a 50% reduction in baseline (BL) PWT after 48 h or on day 14 following nerve injury, then this animal was considered non-allodynic and excluded from the study.

CCI of sciatic nerve

CCI surgery to the left sciatic nerve was performed on all rats as previously described.[22] Under 2% to 3% isoflurane, a small incision was made at the level of the mid-thigh. The sciatic nerve was exposed by blunt dissection through the biceps femoris. Previous studies showed that CCI of sciatic nerve with silk ligatures induced similar infiltration of inflammatory cells and changes in function of the nerve-blood barrier,[23] and more stable neuropathic pain behaviors,[24] as compared to that induced by chromic gut ligature. Accordingly, the nerve trunk proximal to the distal branching point was loosely ligated with four 4-0 silk sutures placed approximately 0.5 mm apart until the epineurium was slightly compressed and minor twitching of the relevant muscles was observed. The muscle layer was closed with 4-0 silk suture, and the wound closed with metal clips.

Electrode placement and SCS treatment

Animals randomized to receive SCS underwent epidural placement of a sterile, quadripolar SCS electrode (Medtronic Inc.) to the dorsal spinal cord (Figure 1(a)). This electrode mimics clinical SCS and was validated in
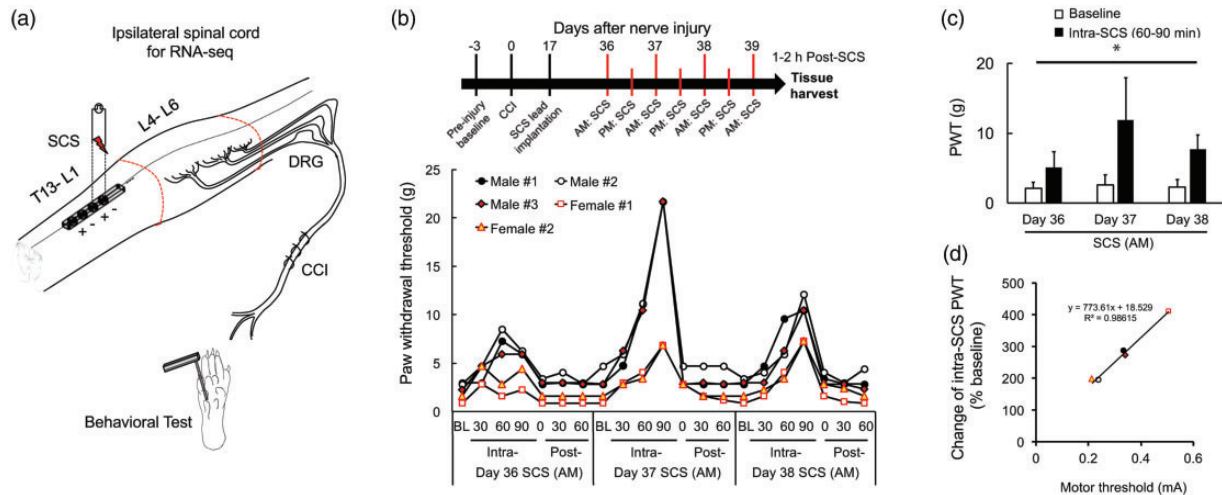
Figure 1. Experimental setup and pain inhibition by SCS. (a) Schematic diagram illustrating the experimental setup. The miniature SCS lead (Medtronic, Minneapolis, MN) was implanted epidurally over the dorsal spinal cord (midline) at the T13-L1 spinal level. Lumbar spinal cord (L4-L6, marked with red lines) tissues ipsilateral to the side of nerve injury were harvest after the last SCS treatment. (b) Upper: Schematic diagram illustrating the experimental timeline. CCI rats ($n = 5$) received the same SCS (red bar, 50 Hz, 80% motor threshold, 0.2 ms, constant current, 120 min/session) from days 36 to 38 post-CCI (two sessions/day) and on day 39 post-CCI (one session). Motor thresholds were measured to 4 Hz stimulation (0.2 ms). Lower: On days 36 to 38 post-CCI, PWTs were measured before (baseline, BL), at 30, 60, and 90 min during SCS (intra-SCS), and at 0, 30, and 60 min after completing SCS in the a.m. session. (c) Average PWTs at 60 and 90 min intra-SCS were significantly increased from pre-SCS baseline on each day. Data are expressed as mean + SD. One-way repeated measures ANOVA. *$p<0.05$ *versus* pre-SCS baseline. (d) To evaluate the peak inhibitory effect of daily SCS on mechanical hypersensitivity in each animal, we averaged PWTs at 60 and 90 min intra-SCS. Then the "Change of intra-SCS PWT" was calculated as follows: Change of intra-SCS PWT = [(mean intra-SCS PWT) − (baseline PWT)]/(baseline PWT) × 100. Scatterplots showed positive linear correlation between change of intra-SCS PWT and motor threshold.
CCI: chronic constriction injury; PWT: paw withdrawal threshold; SCS: spinal cord stimulation; SD: standard deviation.

previous studies in rats.[12,14,18,19] Under isoflurane anesthesia, a laminectomy was performed at the T13 vertebrae level through which the electrode was inserted epidurally in the rostral direction. The position of the electrode was adjusted so that the contacts were at the T13-L1 spinal cord level which corresponds to the lower thoracic-upper lumbar region. Sutures to the muscle were used to secure the electrode in place, and the proximal end was tunneled subcutaneously and exited the animal at the top of its head for later connection to an external neurostimulator (Model 2100, A-M Systems, Sequim, WA).

In "twin-pairs" SCS, the first and third contacts of the lead from rostral were set as an anode (+), and the second and fourth were set as a cathode (−). Conventional SCS (50 Hz, 0.2 ms, constant current, and 120 min/session) was applied at an intensity that activated low-threshold A-fibers (80% motor threshold (MoT)), as described in previous studies.[12,14,18,19] Before SCS, the MoT for each animal was determined by slowly increasing the current amplitude from zero, until muscle contraction in the mid-lower trunk or hind limbs was observed in response to 4 Hz stimulation at 0.2 ms pulse widths. The rats were then acclimated to the testing environment before the pre-SCS BL PWT was measured.

Experimental design

Our primary goal is to examine the changes of gene expression in the spinal cord after repetitive SCS treatments during the maintenance phase of neuropathic pain. All animals developed mechanical hypersensitivity after CCI and were randomized to receive SCS (CCI + SCS group, $n = 8$) or no treatment (CCI only group, $n = 4$). Rats randomized to the CCI+SCS group were implanted with a SCS electrode and received SCS (50 Hz, 80% MoT, 0.2 ms, constant current, 120 min/session, twice per day) for three consecutive days on days 36 to 38 post-CCI (Figure 1(b)). PWTs were measured before BL at 30, 60, and 90 min during SCS (intra-SCS) and at 0, 30, and 60 min after completing SCS in each a.m. session. An additional SCS treatment was given on day 39 post-CCI. Within 1 to 2 h following the last SCS treatment, all animals were euthanized by overdose of isoflurane and decapitation. The ipsilateral lumbar spinal cord (L4-L6 spinal segments) ipsilateral to the nerve lesion was harvested and immediately submerged in DNA/RNA shield solution (Zymo, Irvine, CA) for subsequent RNA extraction. We did not separate the dorsal and ventral half of spinal cord, in order to avoid variations due to different dissections of tissue between different animals.

RNA isolation

Total RNA was extracted from the ipsilateral spinal cord with the Quick-RNA MiniPrep Plus kit (Zymo, Irvine, CA) according to manufacturer instructions with on-column DNase I digestion. RNA quantity was measured by the Qubit RNA BR Assay Kit (ThermoScientific, Waltham, MA), and RNA integrity was assessed by the Bioanalyzer RNA Nano Eukaryote kit on an Agilent 2100 Bioanalyzer (Agilent Technologies, Palo Alto, CA).

RNA-seq library construction and sequencing

Five hundred nanograms of total RNA per sample were used to construct sequencing libraries ($n = 1$ rat/sample). Strand-specific RNA libraries were prepared using the NEBNext Ultra II Directional RNA Library Prep Kit for Illumina (New England Biolabs Inc., Ipswich, MA) after poly(A) selection by the NEBNext poly(A) mRNA Isolation Module (New England Biolabs Inc., Ipswich, MA) according to manufacturer's instructions. Samples were barcoded using the recommended NEBNext Multiplex Oligos (New England Biolabs Inc., Ipswich, MA). Size range and quality of libraries were verified on the Agilent 2100 Bioanalyzer (Agilent Technologies, Palo Alto, CA). RNA-seq libraries were quantified by quantitative polymerase chain reaction using the KAPA library quantification kit (KAPA Biosystems, Wilmington, MA). Each library was normalized to 2 nM and pooled in equimolar concentrations. Paired-end × 150 sequencing was performed on an Illumina HiSeq4000 (Illumina, San Diego, CA). Libraries were pooled and sequenced using two lanes of one HiSeq4000 flow cell to an average depth of 33.6 million reads per sample.

Data analysis

Sequencing reads were aligned to annotated RefSeq genes of the rat reference genome (rn6) using HISAT2,[25] filtered to remove ribosomal RNA, and visualized using the Integrative Genomics Viewer.[26] A gene count matrix that contained raw transcript counts for each annotated gene was generated using the *featureCounts* function of Subread.[27] This count matrix was then filtered for low count genes so that only those genes with >0 reads in each sample were retained. To identify genes that were differentially regulated following SCS, transcript counts were normalized and $\log_2$ transformed using the default normalization procedures in DESeq2.[28] This analysis identified differentially expressed genes between the CCI only and CCI+SCS groups within males or females. The interaction of sex on differential gene expression after injury was evaluated by the interaction term included in the design matrix

within DESeq2. All downstream analyses on RNA-seq data were performed on data obtained from DESeq2. Unless otherwise stated an adjusted *p*-value (i.e., false discovery rate (FDR)) < 0.05 was used to define differentially expressed transcripts between CCI only and CCI+SCS groups. Genes with differential expression between groups were then included in gene ontology (GO) analysis to infer their functional roles and relationships. GO analysis for enriched GO biological processes in each set of differentially enriched genes identified by DESeq2 was performed using ToppGeneSuite (https://toppgene.cchmc.org).[29] The International Union of Basic and Clinical Pharmacology database (http://www.guidetopharmacology.org) was used to assign categories to gene products.[30]

Results

SCS attenuated mechanical hypersensitivity in CCI rats

Rats that developed mechanical hypersensitivity on the ipsilateral hind paw following CCI were randomized to receive SCS (CCI+SCS, $n = 8$) or not receive SCS treatment (CCI, $n = 4$). Following implantation of the SCS electrode on day 17 after CCI, one male and two female rats showed impaired motor function that required exclusion from the study. The remaining five rats (i.e., two female rats, three male rats) that received SCS showed no adverse events, and data from these rats were included in all analyses. Each SCS treatment was associated with increases in mechanical PWT in the ipsilateral hind paw from pre-SCS BL (Figure 1(b)). The peak inhibitory effect of SCS often occurred at 60 and 90 min after start of the SCS and returned to the pre-SCS BL within 30 min of cessation of SCS. The averaged PWTs at 60 and 90 min intra-SCS, which reflect the peak effect of SCS, were significantly increased from pre-SCS BL on each day, $F(3, 16) = 7.47$, $p = 0.024$; Figure 1(c). The change of intra-SCS PWT in individual animals and MoT show a strong correlation, $r(3) = 0.994$, $p < 0.001$, two-tailed test; Figure 1(d).

Differentially regulated genes in the spinal cord after SCS in male and female CCI rats

To determine the effects of SCS on gene expression in the spinal cord that is ipsilateral to the side of nerve injury, we compared RNA-seq data obtained 39 days following CCI to that of rats who received SCS after CCI. Principal component analysis shows segregation of the transcriptomes from CCI rats that received SCS and those that did not receive SCS (Figure 2(a)). The first two principal components accounted for a total of 74%. Compared to CCI only rats, the ipsilateral spinal
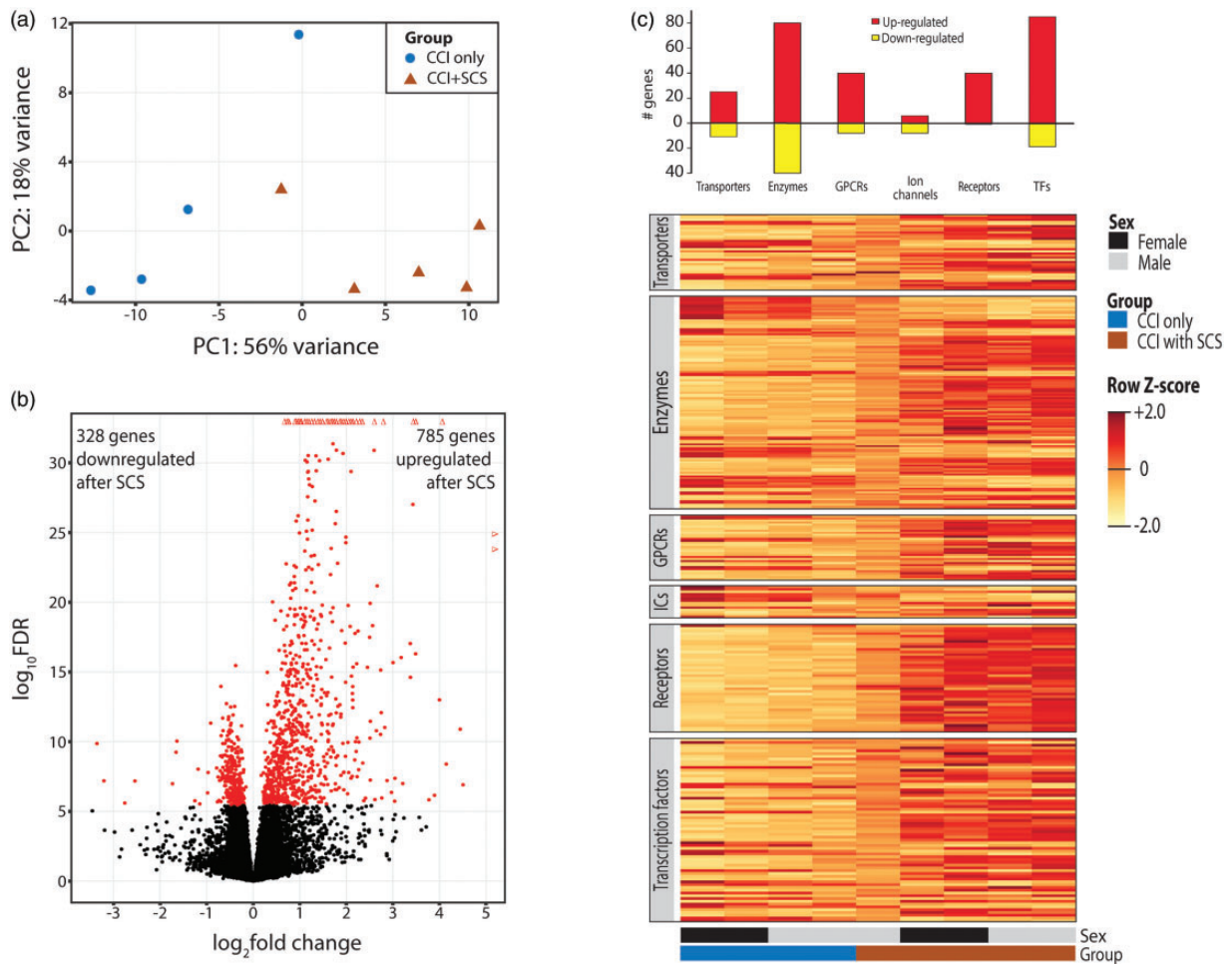
Figure 2. Differential gene expression between CCI rats with and without SCS. (a) Principal component analysis of libraries sequenced for RNA-seq. (b) Volcano plot showing RNA-seq data of ipsilateral L4-L6 spinal cord from CCI rats with and without SCS treatment. DEGs are designated in red and are defined as differentially expressed genes with a FDR < 0.05. Triangles represent genes with extremely high $\log_{10}$FDR or $\log_{2}$fold change values. (c) Bar plot showing the numbers of genes differentially expressed genes up- and downregulated by gene class as defined by the IUPHAR (top). Relative expression levels for each rat are shown for each gene class represented in the bar plot (bottom). Up- and downregulated genes are colored in yellow and orange, respectively. Horizontal bars indicate group assignment and sex for each rat.
CCI: chronic constriction injury; DEG: differentially expressed gene; FDR: false discovery rate; GPCR= G protein-coupled receptor; IC: ion channel; SCS: spinal cord stimulation.

cord from CCI+SCS rats differentially expressed 1113 (7.9%) genes (FDR<0.05; Figure 2(b)). Of these 1113 differentially expressed genes, 785 (70.5%) were upregulated after SCS and 328 (29.5%) were downregulated (Figure 2(b)). The genes most significantly up- and downregulated with SCS treatment are listed in Table 1 and Table 2, respectively. Of the 1113 differentially expressed genes, 343 genes could be classified into gene classes (i.e., transporters, enzymes, G protein-coupled receptors, ion channels, catalytic receptors, and transcription factors) as defined by International Union of Basic and Clinical Pharmacology (Figure 2(c) and Supplemental Figure 1). Mean normalized counts

and relative fold change of specific genes that comprise each of these gene classes is shown in Supplemental Figure 1.

GO analysis of the upregulated genes showed significant enrichment among a variety immune-related biological process (Figure 3(a) and (b)). GO analysis of the downregulated transcripts show significant enrichment among genes involved in synaptic transmission, synaptic organization, and neuron outgrowth (Figure 4(a) and (b)). Molecular functional enrichment analysis identified downregulated differentially expressed genes are involved in protein serine/threonine kinase activity and scaffold protein binding (FDR < 0.005).

Table 1. Top 25 genes upregulated in CCI rats after SCS by FDR.

Ensembl ID	Gene symbol	Full gene name	Log2 fold change	Standard error	FDR
ENSRNOG00000046834	C3	Complement component 3	2.15	0.16	1.77E-35
ENSRNOG00000046254	Adgre1	Adhesion G protein-coupled receptor E1	1.81	0.18	3.16E-19
ENSRNOG00000016294	Cd4	CD4 antigen	1.51	0.16	2.05E-18
ENSRNOG00000004649	Il1b	Interleukin 1-beta	2.46	0.26	1.29E-17
ENSRNOG00000024899	Cxcl13	Chemokine, CXC Motif, Ligand 13	4.07	0.43	1.68E-17
ENSRNOG00000020699	Cd37	Leukocyte surface antigen CD37	1.07	0.12	5.84E-15
ENSRNOG00000013886	Fyb	Fyn-binding protein	1.54	0.18	1.06E-14
ENSRNOG00000008816	Gpnmb	Glycoprotein NMB	1.42	0.17	1.24E-13
ENSRNOG00000050430	Vav1	VAV1 oncogene	1.54	0.19	2.73E-13
ENSRNOG00000042838	Junb	Oncogene JUN-B	1.27	0.16	3.02E-13
ENSRNOG00000008409	Myo1f	Myosin IF	1.38	0.17	6.89E-13
ENSRNOG00000018414	Csf1r	Colony-stimulating factor 1 receptor	1.18	0.15	7.67E-13
ENSRNOG00000043098	Mt2A	Metallothionein 2A	1.89	0.24	7.67E-13
ENSRNOG00000015773	Il21r	Interleukin 21 receptor	2.01	0.25	1.11E-12
ENSRNOG00000038047	Mt1	Matrix metalloproteinase 14	2.28	0.29	1.11E-12
ENSRNOG00000028566	Pld4	Phospholipase D family, member 4	1.16	0.15	1.45E-12
ENSRNOG00000008465	Tmem176b	LR8 protein	1.05	0.13	2.12E-12
ENSRNOG00000042139	Clec4a1	C-type lectin domain family 4, member a1	1.71	0.22	1.63E-11
ENSRNOG00000054964	Aoah	Acyloxyacyl hydrolase	2.60	0.34	2.36E-11
ENSRNOG00000054860	Clec12a	C-type lectin domain family 12, Member A	1.79	0.24	2.36E-11
ENSRNOG00000013564	Dok3	Docking protein 3	1.93	0.26	2.81E-11
ENSRNOG00000021161	Fermt3	Fermentin family (Drosophila) Homolog 3	1.18	0.16	3.07E-11
ENSRNOG00000007350	Rac2	Ras-related C3 Botulinum toxin Substrate 2	1.35	0.18	3.07E-11

FDR: false discovery rate.

Table 2. Top 25 genes downregulated in CCI rats after SCS by FDR.

| Ensembl ID	Gene symbol	Full gene name	Log2 fold change	Standard error	FDR
ENSRNOG00000007112	Pcsk1n	Proprotein convertase subtilisin/kexin type 1 inhibitor	−3.05	0.36	2.93E-14
ENSRNOG00000017932	St3gal2	ST3 beta-galactoside alpha-2,3-sialyltransferase 2	−0.38	0.07	1.62E-05
ENSRNOG00000007573	Hoxb9	Homeobox B9s	−0.69	0.14	5.53E-05
ENSRNOG00000016897	Rlbp1	Retinaldehyde-binding protein 1	−0.57	0.12	1.63E-04
ENSRNOG00000000501	Zfp523	Zinc finger protein 76	−0.40	0.09	1.89E-04
ENSRNOG00000043390	Samd12	Sterile alpha motif domain contain 12	−0.48	0.10	1.96E-04
ENSRNOG00000006649	Thrb	Thyroid hormone receptor beta	−0.43	0.10	3.21E-04
ENSRNOG00000002339	Mark1	Microtubule affinity regulating kinase 1	−0.53	0.12	3.60E-04
ENSRNOG00000004155	Samd14	Sterile alpha motif domain containing 14	−0.66	0.15	3.89E-04
ENSRNOG00000058476	Mast2	Microtubule associated serine/threonine kinase 2	−0.53	0.12	4.24E-04
ENSRNOG00000037793	Cdk5r2	Cyclin-dependent kinase 5 activator 2	−0.48	0.11	5.32E-04
ENSRNOG00000019958	Tmem151b	Transmembrane protein 151B	−0.91	0.21	5.32E-04
ENSRNOG00000009772	Kirrel3	Kin of irregular chiasm-like protein 3	−0.49	0.11	5.99E-04
ENSRNOG00000048980	Gng2	G protein subunit gamma 2	−0.25	0.06	6.09E-04
ENSRNOG00000018526	Dlg4	Discs large MAGUK scaffold protein 4	−0.50	0.12	7.77E-04
ENSRNOG00000023538	Aldh5a1	Aldehyde dehydrogenase 5 family member A1	−0.49	0.11	7.92E-04
ENSRNOG00000013408	Npas2	Neuronal PAS domain protein 2	−0.65	0.15	8.05E-04
ENSRNOG00000016653	Ngef	Neuronal guanine nucleotide exchange factor	−0.46	0.11	8.31E-04
ENSRNOG00000019404	Hhatl	Hedgehog acyltransferase-like	−0.53	0.12	8.52E-04
ENSRNOG00000010938	Slc7a10	Solute carrier family 7 member 10	−0.51	0.12	9.41E-04
ENSRNOG00000008082	Rgs6	Regulator of G protein signaling 6	−0.55	0.13	1.07E-03
ENSRNOG00000008145	Traf3	TNF receptor-associated factor 3	−0.69	0.16	1.07E-03

FDR: false discovery rate.
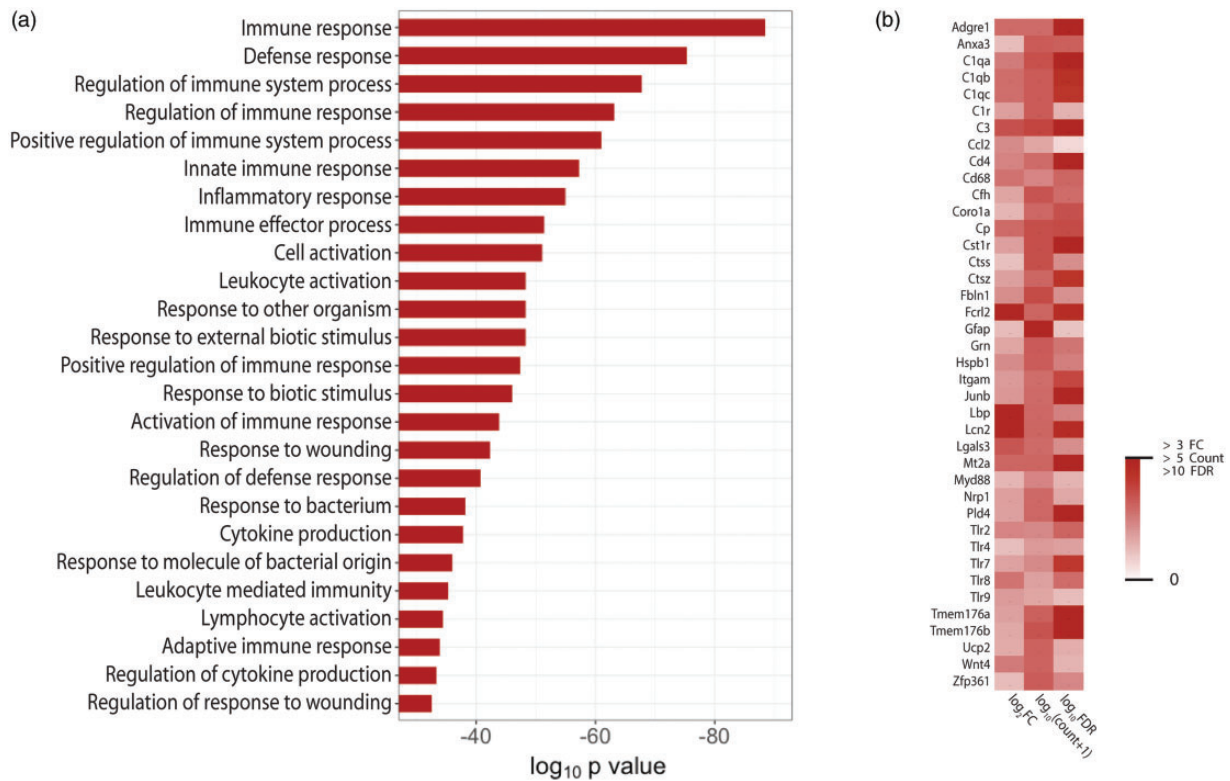
Figure 3. GO biological processes enriched from differentially expressed genes that are upregulated after SCS. (a) The top 25 GO biological processes associated with genes upregulated in CCI+SCS versus CCI only (FDR < 0.05) as ranked by p-value. (b) Heatmap of selected up-regulated genes associated with multiple overrepresented GO biological processes in (a). Data shown are relative expression (i.e., $\log_2 FC$), mean normalized transcript abundance (i.e., $\log_{10}(count+1)$), and statistical significance level (i.e., $\log_{10} FDR$).

Sex differences associated with differentially regulated genes after SCS of CCI rats

Next, we explored sex-specific differential gene expression in the spinal cord associated with repetitive SCS. While both males and females showed a significant increase in PWTs during SCS, the PWTs of the female rats were notably lower than the PWTs of the male rats (Figure 1(b)). To identify sex-specific changes in gene expression associated with SCS treatment, we compared differentially expressed genes between males and females. Following SCS, male CCI+SCS rats differentially expressed 149 genes (Supplemental Figure 2(a)). Of these 149 differentially expressed genes, 28 (18.8%) were downregulated after SCS and 121 (81.2%) were upregulated. GO analysis of the upregulated genes show enrichment in immune and inflammatory pathways (Supplemental Figure 2(b)). In order to perform GO analysis using downregulated genes, we lowered the statistical significance and used the 380 genes which were downregulated after SCS at an unadjusted $p < 0.05$. GO analysis using this subset of genes showed enrichment in genes involved in synaptic signaling (Supplemental Figure 2(b)).

Female CCI + SCS rats differentially expressed 858 genes following SCS at an FDR < 0.05 (Supplemental Figure 2(c)). Of these 858 differentially expressed genes, 192 (22.5%) were downregulated after SCS and 666 (77.5%) were upregulated. Similar to males, GO analysis revealed that the upregulated genes were enriched in immune-related processes and downregulated genes were enriched in synaptic signaling-related processes (Supplemental Figure 2(d)). Hierarchical clustering identified segregation of samples by group and then by sex (Supplemental Figure 2(e)). Two genes (i.e., *Eif2s3* and *Cpne4*) showed significantly increased expression in females versus males at an FDR < 0.05. Expressions of 44 genes were significantly increased in males compared with females (Supplemental Figure 2(f) and Supplemental Table 1).

Discussion

In this study, we identified the effects of multiple sessions of conventional SCS on gene expression in the lumbar spinal cord ipsilateral to the nerve lesion. We administered SCS to rats during the maintenance phase of neuropathic pain using a custom-made quadripolar
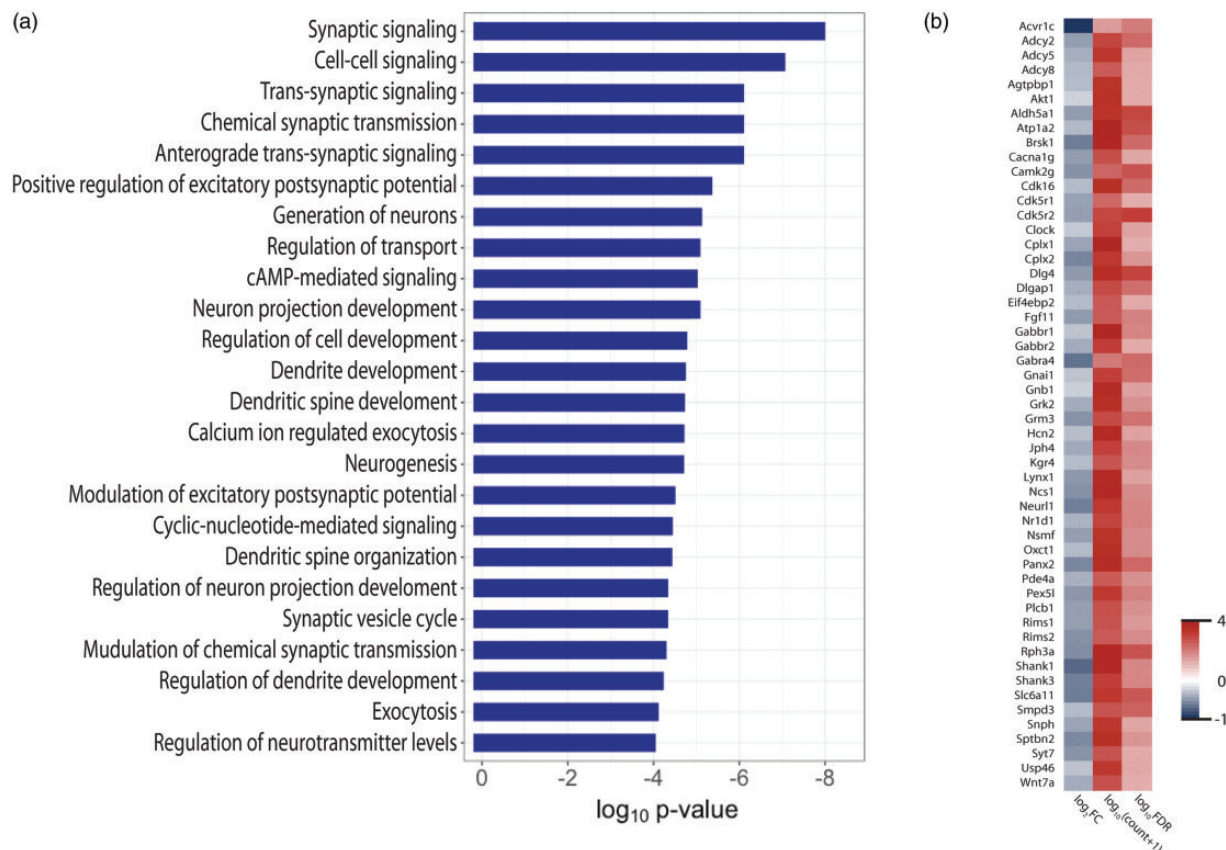
Figure 4. GO biological processes enriched from differentially expressed genes that are downregulated after SCS. (a) The top 25 GO biological processes associated with genes downregulated in CCI+SCS versus CCI only (FDR < 0.05) as ranked by p value. (b) Heatmap of selected downregulated genes associated with the first five overrepresented GO biological processes in (a). Data shown are relative expression (i.e., $\log_2$FC), mean normalized transcript abundance (i.e., $\log_{10}$(count+1)), and statistical significance level (i.e., $\log_{10}$FDR).

electrode, which enabled us to use similar parameters as those used clinically to treat chronic pain.[12,18,19] We chose to use rats that received CCI only as our comparison group in an effort to capture all changes that occur in the spinal cord as a result of surgical implantation of the stimulation electrode and subsequent SCS. Consistent with previous findings,[12,18,19] conventional SCS at the T13-L1 spinal reduced the mechanical hypersensitivity that developed in the ipsilateral hindpaw of CCI rats. The peak inhibitory effect of SCS often occurred 60 to 90 min after starting the SCS. The pain inhibitory effects on each treatment day varied between individual animals and were similar to those observed in other neuropathic pain models.[12,18,19] Pain inhibition by SCS was positively correlated with the MoT. However, the correlation coefficient measures only the degree of linear association between two variables and not causal relationships. Although we included both males and females in our study, we chose to report our analyses after pooling data obtained from both sexes. Only a small number of genes were differentially expressed

between sexes, and male and female rats showed similar GO biological processes associated with SCS (Supplemental Figure 2). Future investigation should include a larger sample size to determine if meaningful differences exist in pain inhibition and gene expression between males and females in response to SCS.[31]

Upregulation of immune-related genes

Following nerve injury, a robust immune response is generated as a result of injury and increased neuronal excitability.[32] Repetitive SCS at T13-L1 was associated with further increases in the expression of immune-related genes in the lumbar spinal cord of CCI rats (Figure 3). These findings are consistent with the only other transcriptome-wide study which reported upregulation of immune-related genes also after SCS.[15] Similarly, SCS was associated with altered expression of proteins involved in a variety of immune-related processes (e.g., wound healing and complement) in cerebrospinal fluid of patients with neuropathic pain.[33] Immune response and gliosis in the spinal cord after nerve injury

are thought to contribute to the maintenance of pathological pain and hyperexcitability of dorsal horn neurons.[34,35] Nevertheless, immune responses can also serve to protect the injured area from further insult, contain pathogens, eliminate damaged cells, and initiate repair mechanisms.[36,37] The physiological implications of increased expression of immune-related genes in the spinal cord after SCS of nerve-injured rats warrant further investigation.

Central sensitization underlying chronic pain is associated with persistent N-methyl-D-aspartate receptor (NMDAR) sensitization to maintain neuronal hyperexcitability as well as the upregulation of toll-like receptors (TLRs).[38,39] To our surprise, in rats with existing CCI to the sciatic nerve, SCS treatment was associated with upregulated TLRs and markers for activated glia. TLR4 is expressed on the cell surface of neurons and immunocompetent cells and can induce a sterile inflammatory response through transcriptional activation of genes that encode key inflammatory mediators (i.e., CCL2/MCP1) as a result of tissue injury/stress.[40] We also found significant upregulation of genes encoding markers for astrocytes (i.e., Gfap and Ccl2) and activated microglia (i.e., Cd68 and Itgam) in the spinal cord following SCS treatments. Activated microglia synthesize and release pro-inflammatory mediators to increase neuronal hyperexcitability following nerve injury.[35] Previous studies have reported conflicting evidence regarding the activation of glia in the spinal cord after SCS. Sato et al.[16] reported decreased glia activation in the spinal cord following 6 h of SCS for four consecutive days as defined by Itgam and Cd68 protein expression. Recently, increased Tlr2 and Cd68 gene expression provided evidence of SCS-induced microglia activation.[15] Our findings are consistent with the latter study. We found upregulation of these genes as well as Gfap which suggests that SCS is associated with increased activation of immune cells in the spinal cord. Whether upregulation of TLRs, glial activation, and immune-related genes may compromise pain inhibition by SCS warrants further investigation.

Downregulation of γ-aminobutyric acid transporters

Despite increased immune responses and glia activation in the spinal cord which may facilitate spinal nociceptive transmission, our animal behavior study found reduction of pain hypersensitivity during each SCS treatment. Thus, the net inhibition of mechanical hypersensitivity by SCS may result from mechanisms other than immune suppression or glial inhibition. The neurochemical mechanisms underlying pain inhibition by conventional SCS include the release of γ-aminobutyric acid (GABA), serotonin, endocannabinoids, acetylcholine, and adenosine into spinal cord.[41–44] Uptake of GABA from the

presynaptic terminals is required to terminate inhibitory neurotransmission by GABA.[45] GAT3 is the GABA transporter expressed on glia that is responsible for the uptake of GABA from the presynaptic terminal and is encoded by Slc6a11. Intriguingly, we found that SCS was associated with decreased expression of Slc6a11. Thus, a decrease of Slc6a11 expression by SCS may be a previously uncharacterized mechanism that promotes pain inhibition through increased availability of GABA within the synaptic cleft.

Downregulation of scaffold genes in the postsynaptic membrane

Changes in synaptic strength between peripheral afferents and second-order neurons underlie central sensitization after nerve injury. This synaptic plasticity is primarily due to activation of NMDAR and localization of α-amino-3-hydroxy-5-methyl-4-isoxazolepropionic acid receptor (AMPAR) to the postsynaptic membrane,[46] which mediate excitatory synaptic transmission of action potentials from peripheral sensory neurons.[47,48] Importantly, we found that several genes involved in neurotransmission and synaptic strength were downregulated in CCI rats following SCS treatment. In particular, among those downregulated were genes encoding scaffold proteins located on the postsynaptic membrane.

The postsynaptic membrane of glutamatergic synapses contains a dense network of proteins known as the postsynaptic density (PSD) that stabilizes glutamatergic receptors localization,[49] prevents lateral diffusion of the receptors in the postsynaptic membrane,[49] and physically links the cytoplasmic domains of receptors to intracellular signaling cascades.[50] Therefore, scaffold proteins within the PSD directly affect synaptic plasticity. Scaffold proteins are generally organized into three layers with each containing a specific family of proteins (e.g., Dlg4, Dlgap1-4, and Shank1-3; Figure 5). First, Dlg4 encodes the Dlg4 protein which binds to the intracellular tails of NMDARs,[51] promotes aggregation of NMDARs and AMPARs in the PSD,[52] and stabilizes AMPAR interactions with its auxiliary proteins.[53] Intrathecal knockdown of Dlg4 expression reduced mechanical and thermal hyperalgesia in rats following L5 spinal nerve ligation.[54,55] In addition, Dlg4-null mice showed decreased glutamate AMPA receptor-mediated synaptic transmission while NMDA receptors were unaffected.[56] Second, Dlgap1-4 encodes four Dlgap proteins which contain domains (i.e., 14 amino acid repeat domains, DLC, GH1) that interact directly with Dlg4 and Shank proteins.[50,57] Altered expression and function of Dlgap proteins is associated with several neurological disorders (e.g., schizophrenia, obsessive compulsive disorder, and autism).[50] Altered Dlgap1-4

gene expression after SCS has not been reported. The third layer contains the Shank family of proteins which are encoded by *Shank1-3*. Shank proteins are large scaffold proteins that contain many protein binding domains which enables them to connect to other Shank proteins, glutamate receptors, signaling proteins, and cytoskeletal proteins.[58] Increased Shank1 protein expression was found after CCI in the ipsilateral dorsal horn.[59] On the other hand, inhibition or siRNA knockdown of *Shank1* in rats after CCI increased mechanical thresholds to pre-injury levels.[60] Our findings are consistent with these studies and suggest that repeated SCS treatment is associated with decreased expression of scaffold proteins that are essential for the stability of NMDA and AMPA receptor aggregation and signaling on the postsynaptic membrane (i.e., *Dlg4, Dlgap1, Dlgap3, Shank1, Shank3, Grip2*; Figure 5). NMDA and AMPA signaling underlies the increased synaptic efficacy indicative of central sensitization. Therefore, destabilization of the PSD may represent a novel mechanism for SCS to result in

inhibition of spinal synaptic transmission and neuropathic pain.

In summary, we showed that gene expression changes in the spinal cord of nerve-injured rats after multiple SCS sessions, and we identify genes and gene networks differentially impacted by conventional SCS under neuropathic pain conditions. Importantly, several key genes that encode scaffold proteins in the PSD are downregulated following SCS which may destabilize the PSD and decrease efficacy of synaptic signaling. The mechanisms leading to changes in gene expression in distal spinal segments after SCS are unknown. During SCS, antidromic action potentials that travel in the dorsal column fibers can reach caudal spinal segments via collateral branches and induce neurochemical changes. SCS may also activate nearby spinal tracts that affect neurons and glial cells in distal spinal segments. Our current findings provide critical insights into transcriptional pathways induced in the spinal cord by repetitive SCS after nerve injury. Future attempts to increase the therapeutic
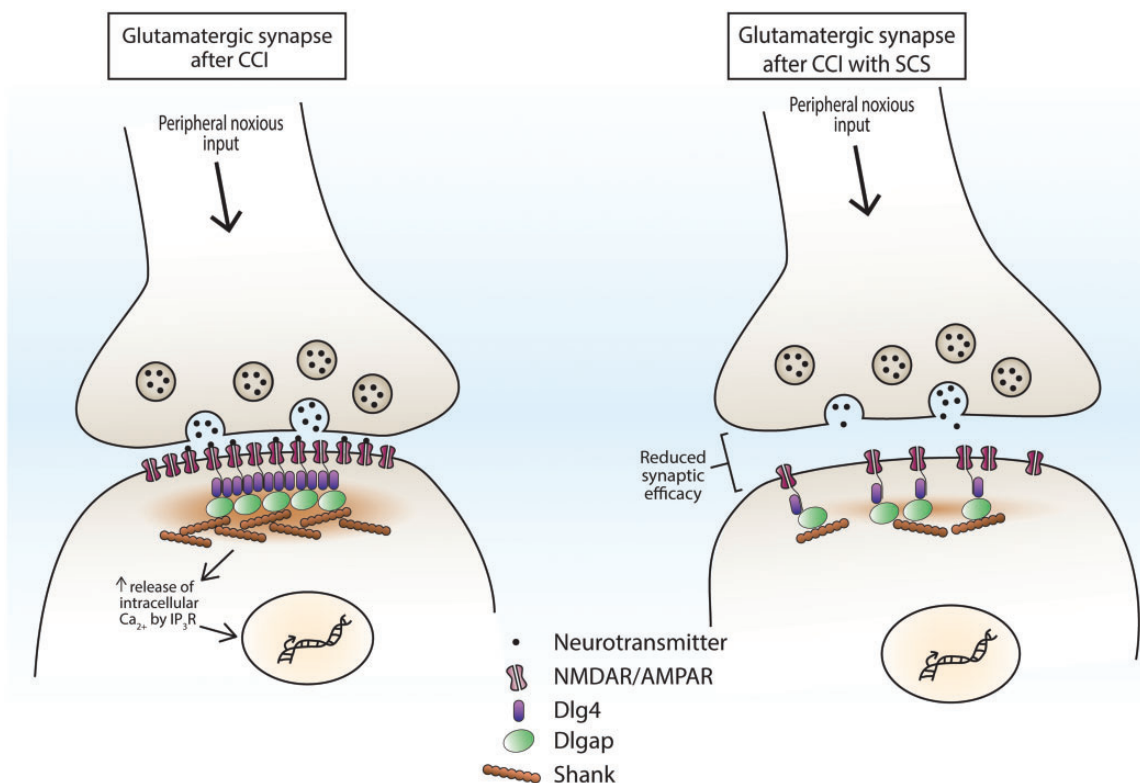

Figure 5. Illustration of a glutamatergic synapse between the central terminal of primary sensory neuron and a post-synaptic dorsal horn neuron with and without SCS. *Left:* Nerve injury increases excitatory synaptic transmission. The organization of the PSD by scaffold proteins facilitates this synaptic plasticity which involves AMPAR localization to the post-synaptic membrane, stabilization of membrane receptors, and physical linkage of the cytoplasmic domains of the receptor to intracellular signaling cascades by Dlg4, Dlgap, and Shank proteins. Activation of these intracellular signaling cascades increases intracellular calcium levels and promotes gene transcription. *Right:* RNA-seq data show downregulation of the scaffold proteins that comprise the PSD (e.g., Dlg4, Dlgap1, Dlgap3, Shank1, Shank3, Grip2), which suggest that repeated SCS treatment is associated with destabilization of the PSD in the spinal cord. Decreased expression of these scaffold genes may reduce NMDAR and AMPAR aggregation at the postsynaptic membrane and hence attenuate excitatory synaptic transmission.

effects of SCS may involve the combination of conventional SCS with other treatments aimed at specific transcriptional and epigenetic targets.

Supplemental material

Supplemental material is available for this article online.

References

1. Kumar K, Taylor RS, Jacques L, Eldabe S, Meglio M, Molet J, Thomson S, O'Callaghan J, Eisenberg E, Milbouw G, Buchser E, Fortini G, Richardson J and North RB. Spinal cord stimulation versus conventional medical management for neuropathic pain: a multicentre randomised controlled trial in patients with failed back surgery syndrome. *Pain* 2007; 132: 179–188.
2. Falowski S and Sharan A. A review on spinal cord stimulation. *J Neurosurg Sci* 2012; 56: 287–298.
3. Deer TR, Mekhail N, Provenzano D, Pope J, Krames E, Leong M, Levy RM, Abejon D, Buchser E, Burton A, Buvanendran A, Candido K, Caraway D, Cousins M, DeJongste M, Diwan S, Eldabe S, Gatzinsky K, Foreman RD, Hayek S, Kim P, Kinfe T, Kloth D, Kumar K, Rizvi S, Lad SP, Liem L, Linderoth B, Mackey S, McDowell G, McRoberts P, Poree L, Prager J, Raso L, Rauck R, Russo M, Simpson B, Slavin K, Staats P, Stanton-Hicks M, Verrills P, Wellington J, Williams K, North R and Neuromodulation Appropriateness Consensus C. The appropriate use of neurostimulation of the spinal cord and peripheral nervous system for the treatment of chronic pain and ischemic diseases: the Neuromodulation Appropriateness Consensus Committee. *Neuromodulation* 2014; 17: 515–550.
4. Krames E, Poree L, Deer T and Levy R. Implementing the SAFE principles for the development of pain medicine therapeutic algorithms that include neuromodulation techniques. *Neuromodulation* 2009; 12: 104–113.
5. Krames ES, Monis S, Poree L, Deer T and Levy R. Using the SAFE principles when evaluating electrical stimulation therapies for the pain of failed back surgery syndrome. *Neuromodulation* 2011; 14: 299–311.
6. Melzack R and Wall PD. Pain mechanisms: a new theory. *Science* 1965; 150: 971–979.
7. Linderoth B and Foreman RD. Conventional and novel spinal stimulation algorithms: hypothetical mechanisms of action and comments on outcomes. *Neuromodulation* 2017; 20: 525–533.
8. Sdrulla AD, Guan Y and Raja SN. Spinal cord stimulation: clinical efficacy and potential mechanisms. *Pain Pract* 2018; 18: 1048–1067.
9. Foreman RD and Linderoth B. Neural mechanisms of spinal cord stimulation. *Int Rev Neurobiol* 2012; 107: 87–119.
10. Linderoth B and Meyerson BA. Spinal cord stimulation: exploration of the physiological basis of a widely used therapy. *Anesthesiology* 2010; 113: 1265–1267.
11. Guan Y, Wacnik PW, Yang F, Carteret AF, Chung CY, Meyer RA and Raja SN. Spinal cord stimulation-induced analgesia: electrical stimulation of dorsal column and dorsal roots attenuates dorsal horn neuronal excitability in neuropathic rats. *Anesthesiology* 2010; 113: 1392–1405.
12. Shechter R, Yang F, Xu Q, Cheong YK, He SQ, Sdrulla A, Carteret AF, Wacnik PW, Dong X, Meyer RA, Raja SN and Guan Y. Conventional and kilohertz-frequency spinal cord stimulation produces intensity- and frequency-dependent inhibition of mechanical hypersensitivity in a rat model of neuropathic pain. *Anesthesiology* 2013; 119: 422–432.
13. Yakhnitsa V, Linderoth B and Meyerson BA. Spinal cord stimulation attenuates dorsal horn neuronal hyperexcitability in a rat model of mononeuropathy. *Pain* 1999; 79: 223–233.
14. Yang F, Xu Q, Cheong YK, Shechter R, Sdrulla A, He SQ, Tiwari V, Dong X, Wacnik PW, Meyer R, Raja SN and Guan Y. Comparison of intensity-dependent inhibition of spinal wide-dynamic range neurons by dorsal column and peripheral nerve stimulation in a rat model of neuropathic pain. *Eur J Pain* 2014; 18: 978–988.

15. Vallejo R, Tilley DM, Cedeno DL, Kelley CA, DeMaegd M and Benyamin R. Genomics of the effect of spinal cord stimulation on an animal model of neuropathic pain. *Neuromodulation* 2016; 19: 576–586.

16. Sato KL, Johanek LM, Sanada LS and Sluka KA. Spinal cord stimulation reduces mechanical hyperalgesia and glial cell activation in animals with neuropathic pain. *Anesth Analg* 2014; 118: 464–472.

17. Tilley DM, Cedeno DL, Kelley CA, Benyamin R and Vallejo R. Spinal cord stimulation modulates gene expression in the spinal cord of an animal model of peripheral nerve injury. *Reg Anesth Pain Med* 2016; 41: 750–756.

18. Yang F, Xu Q, Shu B, Tiwari V, He SQ, Vera-Portocarrero LP, Dong X, Linderoth B, Raja SN, Wang Y and Guan Y. Activation of cannabinoid CB1 receptor contributes to suppression of spinal nociceptive transmission and inhibition of mechanical hypersensitivity by Aβ-fiber stimulation. *Pain* 2016; 157: 2582–2593.

19. Maeda Y, Wacnik PW and Sluka KA. Low frequencies, but not high frequencies of bi-polar spinal cord stimulation reduce cutaneous and muscle hyperalgesia induced by nerve injury. *Pain* 2008; 138: 143–152.

20. Chaplan SR, Bach FW, Pogrel JW, Chung JM and Yaksh TL. Quantitative assessment of tactile allodynia in the rat paw. *J Neurosci Methods* 1994; 53: 55–63.

21. Dixon WJ. Efficient analysis of experimental observations. *Annu Rev Pharmacol Toxicol* 1980; 20: 441–462.

22. Bennett GJ and Xie YK. A peripheral mononeuropathy in rat that produces disorders of pain sensation like those seen in man. *Pain* 1988; 33: 87–107.

23. Yamashita T, Sakuma Y, Kato Y and Kotani J. Effect of different suture materials on the chronic constriction injury model. *J Osaka Dental Universtiy* 2004; 38: 89–94.

24. van der Wal S, Cornelissen L, Behet M, Vaneker M, Steegers M and Vissers K. Behavior of neuropathic pain in mice following chronic constriction injury comparing silk and catgut ligatures. *Springerplus* 2015; 4: 225.

25. Kim D, Langmead B and Salzberg SL. HISAT: a fast spliced aligner with low memory requirements. *Nat Methods* 2015; 12: 357–360.

26. Robinson JT, Thorvaldsdottir H, Winckler W, Guttman M, Lander ES, Getz G and Mesirov JP. Integrative genomics viewer. *Nat Biotechnol* 2011; 29: 24–26.

27. Liao Y, Smyth GK and Shi W. featureCounts: an efficient general purpose program for assigning sequence reads to genomic features. *Bioinformatics* 2014; 30: 923–930.

28. Love MI, Huber W and Anders S. Moderated estimation of fold change and dispersion for RNA-seq data with DESeq2. *Genome Biol* 2014; 15: 550.

29. Chen J, Bardes EE, Aronow BJ and Jegga AG. ToppGene Suite for gene list enrichment analysis and candidate gene prioritization. *Nucleic Acids Res* 2009; 37: W305–W311.

30. Harmar AJ, Hills RA, Rosser EM, Jones M, Buneman OP, Dunbar DR, Greenhill SD, Hale VA, Sharman JL, Bonner TI, Catterall WA, Davenport AP, Delagrange P, Dollery CT, Foord SM, Gutman GA, Laudet V, Neubig RR, Ohlstein EH, Olsen RW, Peters J, Pin JP, Ruffolo RR, Searls DB, Wright MW and Spedding M. IUPHAR-DB: the IUPHAR database of G protein-coupled receptors and ion channels. *Nucleic Acids Res* 2009; 37: D680–D685.

31. Stephens KE, Zhou W, Ji Z, He SQ, Ji H, Guan Y and Taverna SD. Sex differences in gene regulation in the dorsal root ganglion after nerve injury. *bioRxiv*. Epub ahead of print 20 June 2017. DOI: https://doi.org/10.1101/152652

32. Gattlen C, Clarke CB, Piller N, Kirschmann G, Pertin M, Decosterd I, Gosselin RD and Suter MR. Spinal cord T-cell infiltration in the rat spared nerve injury model: a time course study. *Int J Mol Sci* 2016; 17: 352.

33. Lind AL, Emami Khoonsari P, Sjodin M, Katila L, Wetterhall M, Gordh T and Kultima K. Spinal cord stimulation alters protein levels in the cerebrospinal fluid of neuropathic pain patients: a proteomic mass spectrometric analysis. *Neuromodulation* 2016; 19: 549–562.

34. Ben Achour S and Pascual O. Glia: the many ways to modulate synaptic plasticity. *Neurochem Int* 2010; 57: 440–445.

35. Tsuda M. Microglia in the spinal cord and neuropathic pain. *J Diabetes Investig* 2016; 7: 17–26.

36. Jin X and Yamashita T. Microglia in central nervous system repair after injury. *J Biochem* 2016; 159: 491–496.

37. Goldstein EZ, Church JS, Hesp ZC, Popovich PG and McTigue DM. A silver lining of neuroinflammation: beneficial effects on myelination. *Exp Neurol* 2016; 283: 550–559.

38. Ma Q and Woolf C. The NMDA receptor, pain and central sensitization. In: Sirinathsinghji DJS and Hill RG (eds) *NMDA antagonists as potential analgesic drugs*. Basel: Birkhäuser, 2002, pp. 83–103.

39. Schrepf A, Bradley CS, O'Donnell M, Luo Y, Harte SE, Kreder K, Lutgendorf S and Multidisciplinary Approach to the Study of Chronic Pelvic Pain Research N. Toll-like receptor 4 and comorbid pain in interstitial cystitis/bladder pain syndrome: a multidisciplinary approach to the study of chronic pelvic pain research network study. *Brain Behav Immun* 2015; 49: 66–74.

40. Lacagnina MJ, Watkins LR and Grace PM. Toll-like receptors and their role in persistent pain. *Pharmacol Ther* 2018; 184: 145–158.

41. Guan Y. Spinal cord stimulation: neurophysiological and neurochemical mechanisms of action. *Curr Pain Headache Rep* 2012; 16: 217–225.

42. Schechtmann G, Song Z, Ultenius C, Meyerson BA and Linderoth B. Cholinergic mechanisms involved in the pain relieving effect of spinal cord stimulation in a model of neuropathy. *Pain* 2008; 139: 136–145.

43. Song Z, Meyerson BA and Linderoth B. Spinal 5-HT receptors that contribute to the pain-relieving effects of spinal cord stimulation in a rat model of neuropathy. *Pain* 2011; 152: 1666–1673.

44. Cui JG, Linderoth B and Meyerson BA. Effects of spinal cord stimulation on touch-evoked allodynia involve GABAergic mechanisms. An experimental study in the mononeuropathic rat. *Pain* 1996; 66: 287–295.

45. Roth FC and Draguhn A. GABA metabolism and transport: effects on synaptic efficacy. *Neural Plast* 2012; 2012: 805830.

46. Petrenko AB, Yamakura T, Baba H and Shimoji K. The role of N-methyl-D-aspartate (NMDA) receptors in pain: a review. *Anesth Analg* 2003; 97: 1108–1116.

47. Racca C, Stephenson FA, Streit P, Roberts JD and Somogyi P. NMDA receptor content of synapses in stratum radiatum of the hippocampal CA1 area. *J Neurosci* 2000; 20: 2512–2522.

48. Bredt DS and Nicoll RA. AMPA receptor trafficking at excitatory synapses. *Neuron* 2003; 40: 361–379.

49. Bats C, Groc L and Choquet D. The interaction between Stargazin and PSD-95 regulates AMPA receptor surface trafficking. *Neuron* 2007; 53: 719–734.

50. Rasmussen AH, Rasmussen HB and Silahtaroglu A. The DLGAP family: neuronal expression, function and role in brain disorders. *Mol Brain* 2017; 10: 43.

51. Kornau HC, Schenker LT, Kennedy MB and Seeburg PH. Domain interaction between NMDA receptor subunits and the postsynaptic density protein PSD-95. *Science* 1995; 269: 1737–1740.

52. Chen L, Chetkovich DM, Petralia RS, Sweeney NT, Kawasaki Y, Wenthold RJ, Bredt DS and Nicoll RA. Stargazin regulates synaptic targeting of AMPA receptors by two distinct mechanisms. *Nature* 2000; 408: 936–943.

53. Nicoll RA, Tomita S and Bredt DS. Auxiliary subunits assist AMPA-type glutamate receptors. *Science* 2006; 311: 1253–1256.

54. Tao F, Tao YX, Gonzalez JA, Fang M, Mao P and Johns RA. Knockdown of PSD-95/SAP90 delays the development of neuropathic pain in rats. *Neuroreport* 2001; 12: 3251–3255.

55. Tao F, Tao YX, Mao P and Johns RA. Role of postsynaptic density protein-95 in the maintenance of peripheral nerve injury-induced neuropathic pain in rats. *Neuroscience* 2003; 117: 731–739.

56. Beique JC, Lin DT, Kang MG, Aizawa H, Takamiya K and Huganir RL. Synapse-specific regulation of AMPA receptor function by PSD-95. *Proc Natl Acad Sci USA* 2006; 103: 19535–19540.

57. Naisbitt S, Kim E, Weinberg RJ, Rao A, Yang FC, Craig AM and Sheng M. Characterization of guanylate kinase-associated protein, a postsynaptic density protein at excitatory synapses that interacts directly with postsynaptic density-95/synapse-associated protein 90. *J Neurosci* 1997; 17: 5687–5696.

58. Sheng M and Kim E. The Shank family of scaffold proteins. *J Cell Sci* 2000; 113: 1851–1856.

59. Miletic G, Miyabe T, Gebhardt KJ and Miletic V. Increased levels of Homer1b/c and Shank1a in the postsynaptic density of spinal dorsal horn neurons are associated with neuropathic pain in rats. *Neurosci Lett* 2005; 386: 189–193.

60. Miletic G, Dumitrascu CI, Honstad CE, Micic D and Miletic V. Loose ligation of the rat sciatic nerve elicits early accumulation of Shank1 protein in the postsynaptic density of spinal dorsal horn neurons. *Pain* 2010; 149: 152–159.